



Insight into the correlation between the adsorption-transformation behaviors of methylthiophenes and the active sites of zeolites Y



Yun Zu^{a,b}, Yucai Qin^a, Xionghou Gao^{c, **}, Honghai Liu^c, Xiaotong Zhang^a, Jiadong Zhang^a, Lijuan Song^{a,b,*}

^a Key Laboratory of Petrochemical Catalytic Science and Technology, Liaoning Province, Liaoning Shihua University, Fushun 113001, Liaoning, PR China

^b College of Chemistry & Chemical Engineering, China University of Petroleum (East China), Qingdao 266555, Shandong, PR China

^c Lanzhou Petrochemical Research Center, PetroChina Company Limited, Lanzhou 730060, PR China

ARTICLE INFO

Article history:

Received 24 July 2016

Received in revised form 2 October 2016

Accepted 6 October 2016

Available online 6 October 2016

Keywords:

Methylthiophenes

Active sites

Protonation

Oligomerization

Cracking

ABSTRACT

Correlation between the adsorption-transformation behaviors of 2-methylthiophene and 3-methylthiophene and the active sites of NaY, HY and rare earth ion-exchanged ultra-stable Y (REUSY) zeolites have been studied by using an in situ FTIR technique and an intelligent gravimetric analyser-mass spectrometer (IGA-MS) coupling technique. The results show that the bridging hydroxyls (OH) of Si and Al atoms located in the supercage of zeolites Y are the preferred active sites, leading to the protonation and cracking reactions of the methylthiophenes. The AlO^+ active sites in the HY, and the Al(OH)^{2+} and RE(OH)^{2+} active sites in the REUSY both can make the oligomerization reaction occur at 303 and 373 K, and especially, the RE(OH)^{2+} active sites significantly improve the oligomerization abilities. Besides, the activities and selectivities of the protonated 2-methylthiophene and 3-methylthiophene play a decisive role in the oligomerization pathways. As system temperatures of > 473 K, the oligomerization reaction is restricted, while the cracking reaction is improved. Thereby, modulation of the key active sites in adsorbents and system temperatures will be a good prospect for ultra-deep desulfurization in the future.

© 2016 Elsevier B.V. All rights reserved.

1. Introduction

Sulfur concentration in gasolines has been a concerned topic in the worldwide research community due to increasingly stringent environmental regulations and fuel specifications, especially in gasoline. About 85–90 wt.% of the sulfur in gasoline pools originates from fluid catalytic cracking (FCC) naphtha, which accounts for about 35 vol.% to the gasoline pools in USA and West Europe and roughly 80–90 vol.% in China [1–3].

In the FCC naphtha, short chain alkylthiophenes, especially methylthiophenes and dimethylthiophenes, can be detected using different detected techniques, e.g. GC-PFPD, GC-SCD, and GC-AED, etc., and are considered as the major sulfur compounds in the fuels [4–6]. Possible pathways about the origin of these sulfur compounds have been proposed [7,8]. The direct one is the cracking of heavy sulfur-containing molecules present in FCC feedstocks. Another possibility is the reaction of large amounts of H_2S with

the olefins or diolefins resulting from the cracking of hydrocarbon of the feedstocks.

In recent years, some possible processes have been being developed for ultra-deep desulfurization of FCC naphtha, such as selective adsorption desulfurization (SADS), olefins alkylation of thiophenic sulfur (OATS), oxide desulfurization (ODS), and in situ sulfur removal in FCC process, etc. [9–11]. Surprisingly, the methylthiophenes still account for the main proportion among all sulfur compounds in the treated FCC naphtha [9,12]. The removal of the methylthiophenes comes into being, therefore, an inevitable challenge.

Currently, the interaction between the methylthiophene molecules and the adsorbents is the essential problem for meeting the challenge. In the SADS process, for example, numerous researcher has been devoted to research Lewis acidic center of the zeolite-based sorbents (Cu(I)Y , Ni(II)Y , Ag(I)Y , and CeY , etc.), in which the methylthiophene molecules adsorbed on the sorbents through different adsorptive modes (e.g. π -complexation and “S-M” interaction) [13–16]. However, Brønsted acidic center located in the sorbents have been ignored, which can result in the occurrence of some catalytic conversion reactions of thiophenic sulfur compounds, such as protonation, oligomerization, and cracking reactions [17–19]. A similar conclusion can be obtained that the

* Corresponding author at: Key Laboratory of Petrochemical Catalytic Science and Technology, Liaoning Province, Liaoning Shihua University, Fushun 113001, Liaoning, PR China.

** Corresponding author.

E-mail addresses: zuyun1990@126.com (Y. Zu), gaoxionghou@petrochina.com.cn (X. Gao), lsong56@263.net (L. Song).

effect of the Lewis acidic center have been neglected in the in situ sulfur removal in FCC process, or the OATS process [20–22].

Subsequent studies, therefore, are devoted to explore the synergistic effect between Brönsted and Lewis acidic centers in acidic catalysts that become an inevitable and important factor for sulfur reduction in FCC process. Pang et al. [23] studied the modification of USY zeolite with Zn, V, Cu and RE, which modulated simultaneously the acidity of Brönsted acid and Lewis acid. Results have shown that the USY modified with the combination of RE and V yielded the superior catalyst that showed both high sulfur reduction performance and desirable product selectivity. Potapenko et al. [24,25] also have found that hydrogen transfer reactions as main reaction pathways of thiophenic sulfur compounds, can be promoted by Brönsted (zeolites additives) and Lewis (spinel additives) acidic active sites in reducing the sulfur content in FCC naphtha. In our previous work [17,26], we have concluded that Lewis acidic center associated with cerium (Ce) ions species, combining with Brönsted acidic center in CeY zeolite, can prompt the oligomerization and cracking reactions of thiophenic sulfur compounds.

The abovementioned studies, however, still stay in the Brönsted/Lewis acidic centers with generalized and macroscopic level, and cannot explicitly clarify what roles of the active sites play in the adsorption-transformation behaviors of the sulfur compounds in FCC naphtha. According to the literatures reported [27–30], the acidity of Brönsted acidic site can be simultaneously influenced by the types and location of related ions species, such as extra-framework aluminum (EFAL) species (AlOOH , Al(OH)_3 , Al(OH)^{2+} , or AlO^+ , etc.). Li et al. [27,28] have found that, for example, extra-framework aluminum Al(OH)_3 and Al(OH)^{2+} species in the supercage cage and Al(OH)^{2+} species in the sodalite cage are the preferred Lewis acidic sites, which could enhance the acidity of the nearest Brönsted acidic site in the HY by the DFT method. Similarly, the formation of the metal ions species (Cu^+ , Ni^{2+} , Ag^+ , and RE^{3+} , etc.) during the modification of adsorbents, also can affect the acidity of Brönsted acidic site [14,31–33]. Meanwhile, the abovementioned metal ions species can constitute different active sites by itselfs, which have been conformably considered as Lewis acidic centers in previous papers.

To date, however, no detailing reports are mentioned to comprehensively and deeply investigate the correlation between adsorption-transformation behaviors of the methylthiophenes and each active site in catalysts and/or adsorbents; that is, each step reaction of the methylthiophene molecules on which active site is unclear, mainly due to the complexities and ambiguities of each active site in the adsorbents. Thus, it is reasonable to assume that all the active sites in the adsorbents can play a decisive role in deeply removing the methylthiophenes, which is worth us to ponder over.

The primary objective of the present work was to reveal the correlation between adsorption-transformation behaviors of 2-methylthiophene and 3-methylthiophene and the active sites of NaY, HY and rare earth ion-exchanged ultra-stable Y (REUSY) zeolites using an in situ FTIR technique and an intelligent gravimetric analyser-mass spectrometer (IGA-MS) coupling technique, in view of a possible improvement of the catalytic cracking catalysts and/or adsorbents and to design an effective method to reduce the content of the methylthiophenes, or even thiophenic sulfur compounds in FCC naphtha.

2. Experimental

2.1. Adsorbents and reagents

The commercial NaY and HY zeolites were supplied by Catalyst Plant of NanKai University Ltd., China and the commercial rare earth ion-exchanged ultra-stable Y (REUSY) was provided by Catalyst

Plant of Lanzhou Petrochemical Company, PetroChina Company, Ltd. Pyridine, 2-methylthiophene and 3-methylthiophene were purchased from J&K Ltd., with a purity of 99%. Sodium hydroxide with a purity of 99% and toluene with a purity of 98% were both supplied by Sinopharm Chemical Reagent Ltd., China.

2.2. Adsorbent characterization

X-ray powder diffraction (XRD) patterns were collected in a 2θ range of 5–60° using a D/MAXRB XRD instrument (Rigaku, Japan) equipped with $\text{CuK}\alpha$ radiation.

Surface area and pore volume of the samples were examined by nitrogen adsorption-desorption at -196°C on a ASAP 2020 micropore size analyzer (Micromeritics). The acidity of the samples was determined by using pyridine-Fourier transform infrared (Py-FTIR) (Perkin-Elmer, Spectrum TM GX) and thermoproduced desorption of ammonia (NH_3 -TPD) (Micromeritics, Auto Chem II Chemisorption Analyzer) method.

2.3. *in situ* Fourier transform infrared spectroscopy (*in situ* FTIR)

Adsorption and transformation behaviors of 2-methylthiophene and 3-methylthiophene over the zeolite-based sorbents (NaY, HY and REUSY) were studied by using an *in situ* FTIR technique. Prior to the measurement, the self-supporting wafer (*ca.* 0.01 g) of the sorbents were activated in an *in situ* cell under a vacuum of $< 10^{-3}$ Pa at 673 K for 3 h. The adsorbates (2-methylthiophene, 3-methylthiophene) were, then, dosed into the sorbents up to adsorption saturation at 303 K . The FTIR spectra were scanned between 4000 and 400 cm^{-1} with 4 cm^{-1} spectral resolution and 64 scans after the adsorbed sorbents degassed at temperatures of 303 , 373 , 473 , and 573 K for 0.5 h, respectively, using a Perkin-Elmer Spectrum TM GX spectrometer.

The correlation between adsorption behaviors of the methylthiophenes and the active sites of the zeolites Y (HY, REUSY) were further studied by the *in situ* FTIR technique in which the methylthiophenes were dosed into the *in situ* cell with different concentrations, from low to high in turn, at 303 K for 0.5 h. The FTIR spectra were scanned after the adsorbed sorbents degassed at 303 K for 0.5 h for each dose. The vacuum pressure and the other experiment conditions were the same to the above *in situ* FTIR experiments.

2.4. Temperature programmed desorption-dynamic mass spectrometer (TPD-DMS)

An intelligent gravimetric analyser-mass spectrometer (IGA-MS) coupling technique provided by Hiden Analytical Ltd. (Warrington, UK), was used to carry out the temperature programmed desorption (TPD) measurements for the methylthiophenes adsorbed in the NaY, HY and REUSY. The sorbents (*ca.* 0.15 g) were put into a sample boat and outgassed under a vacuum of $< 10^{-5}$ Pa at 673 K for 3 h prior to the sorption measurement. The adsorbates (2-methylthiophene, 3-methylthiophene) were, then, adsorbed on the sorbents, after the sorbents naturally cooled down to 303 K , until an adsorption equilibrium was obtained. The adsorbed saturation sorbents were, then, degassed from 303 to 773 K with a heating rate of 10 K min^{-1} . The above equilibrium pressure was maintained during the heating. The weights of the sorbents were recorded as a function of temperature from which Thermal Gravimetry (TG) and Differential Thermal Gravimetry (DTG) profiles could be derived. Meanwhile, the signal change of the desorbed products, which was qualitatively determined from the mass to charge ratio displayed through the Bar-mode of the MS, was detected through the Mid-mode of the MS.

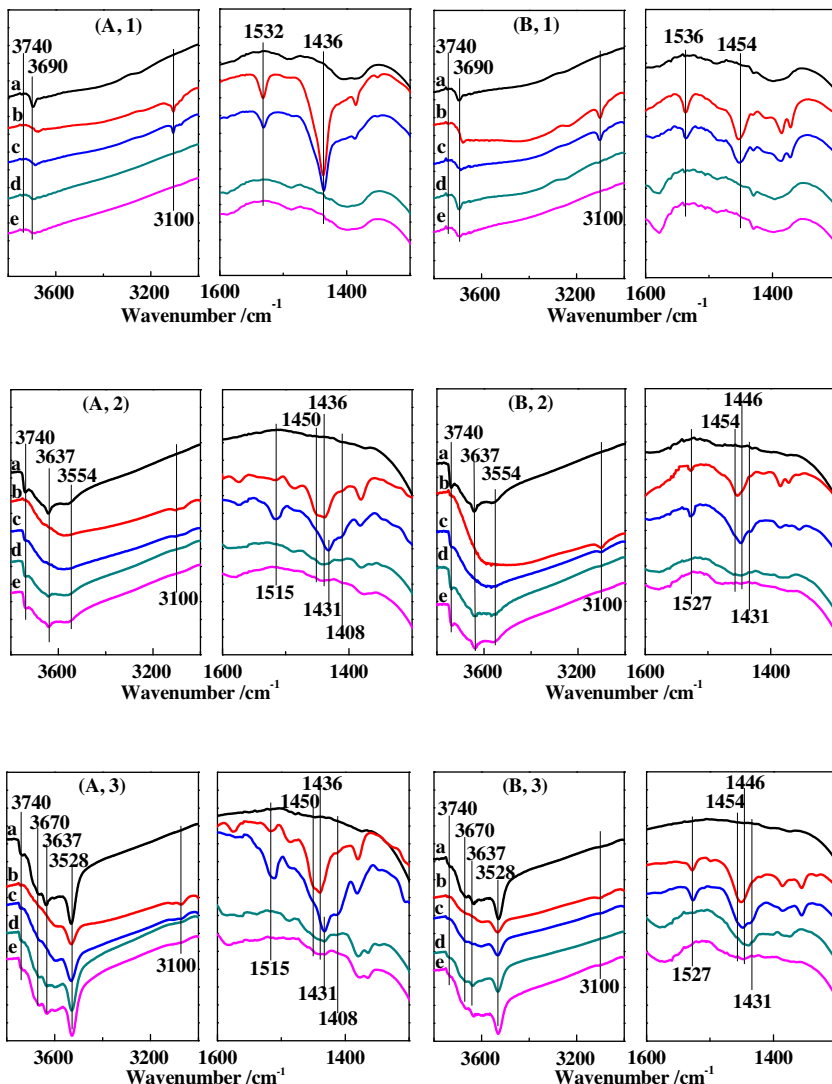


Fig. 1. In situ FTIR spectra of 2-methylthiophene (A) and 3-methylthiophene (B) adsorbed on the NaY (1), HY (2) and REUSY (3) at 303 K and at degassing temperatures of 303 K (b), 373 K (c), 473 K (d), 573 K (e); the each top line (a) represents the background spectra of the samples.

2.5. Sulfur compounds species analysis by GC-SCD/GC-MSD

Probable general and structural formulas of the sulfur compounds species trapped on the zeolites Y were analyzed by a method that the adsorbed saturation samples were dissolved in a solution of NaOH (4 mol L⁻¹) and toluene (10 ml) at 323 K for 1 h. The upper products in the tube after the centrifugalization of the mixed solution, were analyzed on a PerkinElmer Clarus 500 gas chromatography-sulfur chemiluminescence detector (GC-SCD) equipped with a chromatographic column HP-PONA (50 m × 0.200 mm × 0.5 μm) and on a Agilent 7890A/5975C gas chromatography-mass spectrometry detector (GC-MSD) equipped with a chromatographic column HP-5 ms (30 m × 0.250 mm × 0.25 μm), respectively. The weight of the sorbents was the same before the each adsorptive experimental process.

3. Results and discussion

3.1. in situ FTIR study on adsorption behaviors

The FTIR spectra of 2-methylthiophene and 3-methylthiophene adsorbed on the NaY are given in Fig. 1(A, 1) and (B, 1). The

bands at 3100, 1532 and 1436 cm⁻¹ for 2-methylthiophene, and the bands at 3100, 1536 and 1454 cm⁻¹ for 3-methylthiophene, are observed at degassing temperatures of 303 and 373 K (cf. Fig. 1(A, 1) and (B, 1), lines b and c). Among them, the band at 3100 cm⁻¹ is assigned to the C–H stretching vibrations of the thiophene-ring of 2-methylthiophene and 3-methylthiophene. The bands at 1532 and 1536 cm⁻¹ are ascribed to the fundamental ring stretching vibrations of the methylthiophene molecules. Remarkably, the characteristic absorption peaks of 1436 and 1454 cm⁻¹ attributed to the asymmetric variable angle vibrations of the methyl groups (CH₃) of the adsorbed 2-methylthiophene and 3-methylthiophene molecules, respectively, shift to lower wavenumbers (red-shift), compared to the corresponding absorption peaks of pure 2-methylthiophene and 3-methylthiophene. This red-shift phenomenon can be attributed to a decrease in the electron density of the entire thiophene-ring, implying that the thiophene-ring of the adsorbed methylthiophene molecules is parallel to the surface of the sorbent, that is, the methylthiophene molecules are adsorbed onto the Na⁺ active sites in the NaY by π electron interaction. The Na⁺ active sites correspond to the band at 1442 cm⁻¹ in the Py-FTIR spectra of the NaY (cf. Fig. S3). This phenomenon is similar to the red-shift of the band at 1396 cm⁻¹ in the FTIR spectra of thiophene adsorbed on the NaY [16,34]. Fur-

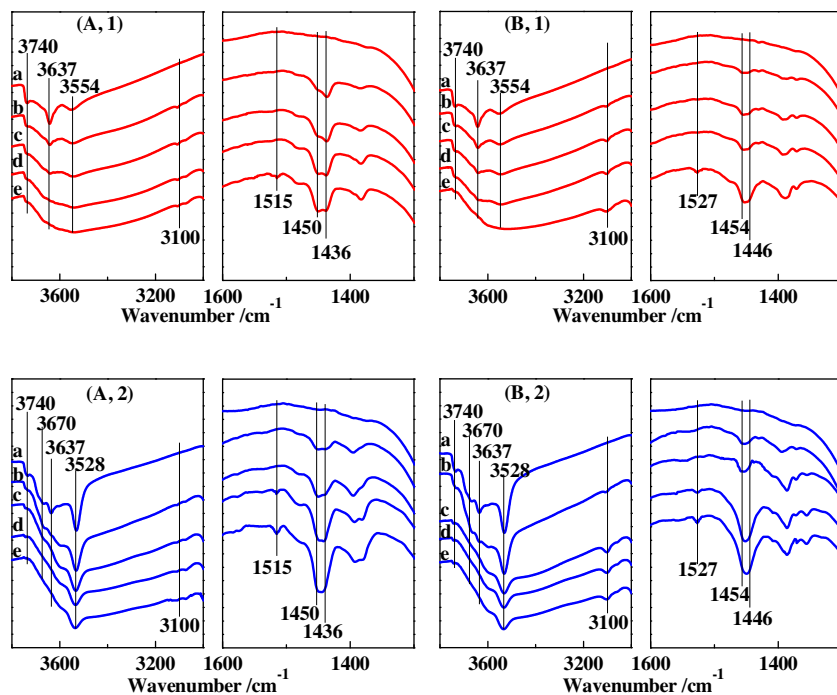


Fig. 2. In situ FTIR spectra of 2-methylthiophene (A) and 3-methylthiophene (B) adsorbed on the HY(1) and REUSY(2) at 303 K with different concentrations from low (b) to high (e) in turn and then degassed at 303 K for each dose; the each top line (a) represents the background spectra of the samples.

thermore, the adsorbed methylthiophene molecules on the NaY can be desorbed thoroughly at degassing temperature of 473 K (cf. Fig. 1(A, 1) and (B, 1), line d), implying that the interaction of the above adsorptive mode is relative weak.

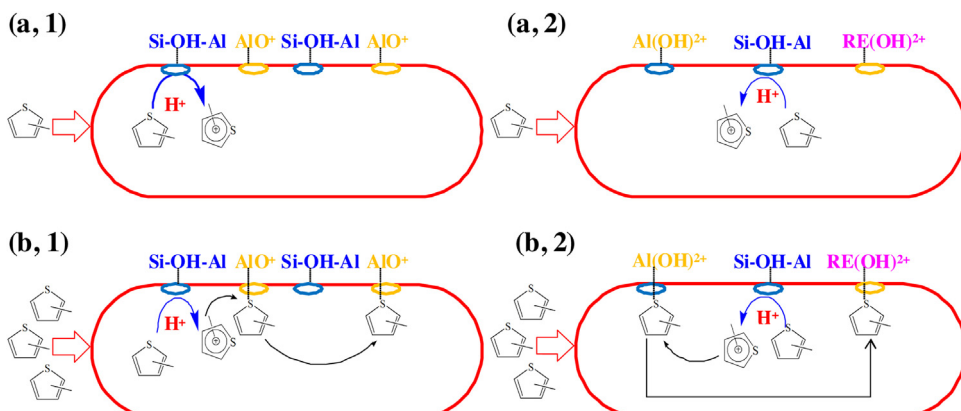
The FTIR spectra of 2-methylthiophene and 3-methylthiophene adsorbed on the HY and REUSY are presented in Fig. 1(A, 2), (A, 3), (B, 2) and (B, 3). Noteworthily, some new infrared bands appearing at 1408, 1455 and 1515 cm⁻¹ for 2-methylthiophene, and 1431, 1446 and 1527 cm⁻¹ for 3-methylthiophene adsorbed on the HY and REUSY, respectively, are observed (cf. Fig. 1(A, 2), (A, 3), (B, 2) and (B, 3), line b). The new infrared bands at 1455 and 1446 cm⁻¹ can be assigned to the deformation vibrations of methylene groups (CH₂) of the protonated 2-methylthiophene and 3-methylthiophene, respectively, as reported by Hogeveen [35], indicating that the protonation reaction of the methylthiophene molecules occurs on both the HY and REUSY. More interestingly, like the new band at 1504 cm⁻¹ related to the thiophene oligomers as the thiophene adsorbed on CeY, or LaNaY, etc. [16,17], the new infrared bands of 1515 and 1527 cm⁻¹ (ring stretching fundamental) can be associated with the 2-methylthiophene and 3-methylthiophene oligomers, respectively, suggesting that the oligomerization reaction of the methylthiophene molecules takes place on both the HY and REUSY, as well. Combining with the above conjecture, the new band at 1408 cm⁻¹ in the FTIR spectra of 2-methylthiophene and the new band at 1431 cm⁻¹ in the FTIR spectra of 3-methylthiophene are also associated with the methylthiophene oligomers, which are possibly assigned to the blending vibrations of CH₂ groups of the methylthiophene oligomers. The probable general and structural formulas of the 2-methylthiophene and 3-methylthiophene oligomers have been provided in the subsequent sections by using the GC-SCD and GC-MS coupling techniques (cf. Figs. 3 and 4).

Further, the abovementioned bands take place with different degrees of changes on the HY and REUSY, as the degassing temperature is up to 373 K, especially those new absorption peaks discussed above (cf. Fig. 1(A, 2), (A, 3), (B, 2) and (B, 3), line c). The bands at 1436 and 1454 cm⁻¹ weaken obviously, implying

that most adsorbed methylthiophene molecules may be desorbed from the HY and REUSY, or converted into more stable methylthiophene species. In particular, for 2-methylthiophene, the band at 1455 cm⁻¹ weaken, and the bands of 1408 and 1515 cm⁻¹ strengthen, and moreover, a new strong absorption peak of the band at 1431 cm⁻¹ appear. For 3-methylthiophene, however, the band at 1446 cm⁻¹ strengthen obviously, but the bands at 1431 and 1527 cm⁻¹ strengthen slightly, compared to the relevant bands (1408 and 1515 cm⁻¹) of the 2-methylthiophene oligomers. The strengthening of the bands appearing at 1408, 1431, 1515 and 1527 cm⁻¹ implies that the oligomerization reaction of the methylthiophene molecules occurs further, and then the relatively stable methylthiophene oligomers may be formed. Notably, the oligomerization abilities of 2-methylthiophene adsorbed on the HY and REUSY are more stronger than that of 3-methylthiophene. On the contrary, 3-methylthiophene molecules mainly tends to occur the protonation reaction further. These obvious difference are directly due to the CH₃ groups position of 2-methylthiophene and 3-methylthiophene. The nearer the S atoms close to the CH₃ groups position, the easier the proton (H⁺) in the adsorbents devoting to attack the 2- or 5-position of the methylthiophene molecules where have higher density of electron cloud [35], eventually can improving the protonation and oligomerization abilities.

With the degassing temperature rising further, most bands disappear except for the broad adsorption peaks in the range of 1431–1455 cm⁻¹ for 2-methylthiophene, and 1431–1454 cm⁻¹ for 3-methylthiophene (cf. Fig. 1(A, 2), (A, 3), (B, 2) and (B, 3), lines d and e), implying that the desorption of the methylthiophene oligomers adsorbed on the adsorbent surface is not a simple process, but a relative complex catalytic conversion process, and the catalytic reaction contributes to the cracking of the methylthiophene oligomers.

Interestingly, however, whatever 2-methylthiophene or 3-methylthiophene molecules adsorbed on the REUSY both displays the stronger intensities of the relevant bands discussed above than that on the HY, especially when the degassing temperature is at 303 and 373 K, evidently indicating that the protonation and oligomer-



Scheme 1. Schematic diagram of the methylthiophene molecules adsorbed on the active sites in the HY (1) and REUSY (2) with low (a) and high (b) concentrations.

ization abilities of the methylthiophene molecules are more violent on the REUSY.

Therefore, in order to get a deep insight into the protonation and oligomerization microscopic processes of the methylthiophene molecules on the HY and REUSY, Fig. 2 displays the FTIR spectra of 2-methylthiophene and 3-methylthiophene adsorbed on the HY and REUSY by dosing the methylthiophene molecules with different concentrations slowly from low (b) to high (e) in turn. It can be observed that, in the FTIR spectra, special attention should be paid to the changes of the bands assigned to each active site in the HY and REUSY, and the corresponding protonation and oligomerization reactions on those active sites. Fig. S3 provides the detail assignment of the bands, corresponding to different active sites, respectively. The bands at 3740 and 3637 cm⁻¹ are assigned to the terminal silanol (Si-OH) active sites, and the bridging hydroxyl (OH) active sites of Si and Al atoms located in the supercage of zeolites Y, respectively. The bands at 3670 and 3528 cm⁻¹ are attributed to the extra-framework aluminium hydroxyl [Al(OH)²⁺] and rare earth ions species [RE(OH)²⁺] active sites in the REUSY, respectively. Furthermore, for the HY, the bands at 3554 and 1455 cm⁻¹ are assigned to the OH active sites of Si and Al atoms located in the sodalite cage and extra-framework aluminium (AlO⁺) active sites, respectively.

Notably, the band at 3637 cm⁻¹ has become weak obviously under the lower concentration (cf. Fig. 2, line b). However, there is no obvious change for the other bands. Correspondingly, the bands of 1455 and 1446 cm⁻¹ have been observed, prior to the appearance of the bands of 1515 and 1527 cm⁻¹, indicating that the protonation reaction of the methylthiophene molecules occurs preferentially, and then the oligomerization reaction starts to take place. This result fully indicates that the OH active sites of the Si and Al atoms located in the supercage of the HY and REUSY are the preferred active sites in the oligomerization reaction, interacted with the low content of the methylthiophene molecules (cf. Scheme 1, a).

With the concentrations increasing further (cf. Fig. 2, line e), the AlO⁺ active sites located in the HY, are covered, except for a few OH active sites of the Si and Al atoms located in the sodalite cage that are less inaccessible. For the REUSY, not only the Al(OH)²⁺ active sites are occupied entirely, but also a few RE(OH)²⁺ active sites located in the sodalite cage are covered, as well. Meanwhile, the bands at 1515 and 1527 cm⁻¹ can be detected. These findings indicate that only when some methylthiophene molecules begin to adsorb on the AlO⁺ active sites in the HY, or the Al(OH)²⁺ and RE(OH)²⁺ active sites in the REUSY, the oligomerization reaction can take place after the occurrence of the protonation of the methylthiophene molecules (cf. Scheme 1, b). Hence, the requirement of the oligomerization reaction can be inferred that it can be able to collide

each other between the protonated methylthiophene molecules and the adjacent adsorbed methylthiophene molecules.

Observingly, the bands of 1515 and 1527 cm⁻¹ are detected preferentially when the methylthiophene molecules adsorb on the REUSY, compared to that on the HY under the same concentration (cf. Fig. 2, line d), confirming that the oligomerization reaction of the methylthiophene molecules on the REUSY occurs more easily than that on the HY. It can be known, therefore, that the adsorptive abilities and modes between the RE(OH)²⁺ active sites and the methylthiophene molecules are conducive to prompt the oligomerization reaction, compared to only weak adsorptive active sites (AlO⁺) in the HY. Consequently, the oligomerization abilities can be affected by the adsorptive abilities and modes of those active sites in the zeolites, and the concentrations of the methylthiophene molecules.

3.2. Oligomerization mechanisms

For purpose of getting a visual and comprehensive understanding for the formation and transformation processes of the methylthiophene oligomers on the active sites in the HY and REUSY, the sulfur compounds species trapped on the HY and REUSY are confirmed in Fig. 3 by using the GC-SCD coupling technique. The qualitative analysis of these sulfur compounds is shown in Fig. 4 by employing the GC-MS coupling technique and combining with the NIST database. All the probable general and structural formulas of these sulfur compounds are listed in Table 2S.

In the systems of 2-methylthiophene and 3-methylthiophene adsorbed on the HY and REUSY at 303 K, the 2-methylthiophene trimers (cf. Fig. 3, k1 and k2) and the 3-methylthiophene trimers (cf. Fig. 3, k3 and k4) are detected in the GC-SCD chromatograms and the corresponding qualitative analysis results are obtained by the GC-MS (cf. Fig. 4, III, IV, V, and VI), which is consistent with the appearance of the bands at 1515 and 1527 cm⁻¹ in the FTIR spectra of the methylthiophene molecules on the samples (cf. Fig. 1(A, 2), (A, 3), (B, 2) and (B, 3), line b). In previous studies, the methylthiophene trimers have been found by Meisel et al. [36] when the 3.0 mol of the methylthiophene molecules were added 10 g of phosphorus pentoxide and 25 g of 85% orthophosphoric acid during the temperature rose from 357 to 369 K for 6 h and their probable chemical structure have been inferred by Ishigaki et al. [37]. In this work, it can be seen that the content of the trimers on the REUSY is slightly higher than that on the HY, well confirming that the RE(OH)²⁺ active sites in the REUSY can significantly improve the oligomerization abilities of the methylthiophene molecules, compared to that on the HY. Moreover, the content of the 2-methylthiophene trimers is obviously more than that of the 3-methylthiophene trimers, indicating that the oligomerization abilities of 2-methylthiophene are

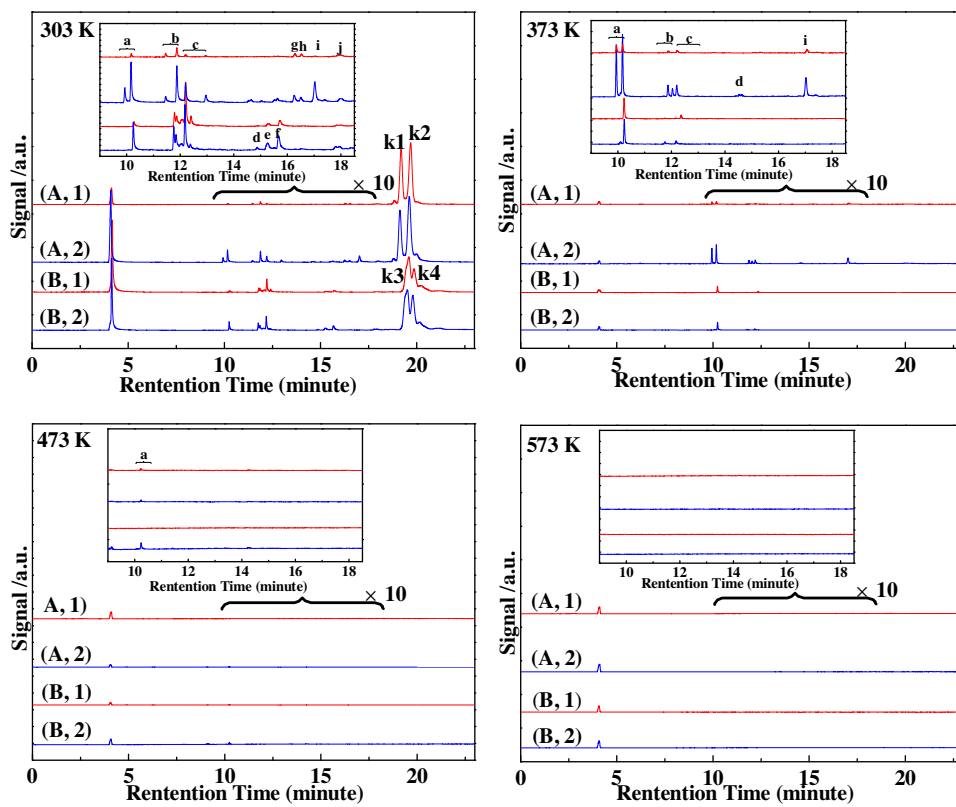


Fig. 3. GC-SCD chromatograms of the sulfur compounds species trapped on the HY (1) and REUSY (2) zeolites after interacting with 2-methylthiophene (A) and 3-methylthiophene (B) at certain temperatures of 303, 373, 473 and 573 K. Probable general and structural formulas of the sulfur compounds species a, b, c, d, e, f, g, h, i, j, k1, k2, k3, and k4 are listed in Table 2S. Inset denotes areas being magnified 10 times.

evidently stronger than that of 3-methylthiophene, which verifies the conclusion in the FTIR spectra discussed above (*cf.* Fig. 2). Besides, for the 2-methylthiophene trimers, the content of the k2 sulfur compound is slightly higher than that of the k1 sulfur compound, and for the 3-methylthiophene trimers, a similar result can be found that the content of the k3 sulfur compound is slightly higher than that of the k4 sulfur compound. Most possibly, the steric hindrance of the 2-methylthiophene or 3-methylthiophene trimers in the oligomerization process can be used to explain the results.

In summary, the abovementioned results well reveal the correlation between the protonation and oligomerization microscopic processes of the methylthiophene molecules and each active site in the HY and REUSY. Initially, the OH active sites of the Si and Al atoms located in the supercage of the HY and REUSY are occupied preferentially by 2-methylthiophene and 3-methylthiophene molecules, and the corresponding protonation reaction occurs. Subsequently, the methylthiophene molecules display the stronger protonation abilities on the REUSY, mainly due to the stronger acidity and lower density of the OH active sites of the Si and Al atoms located in the supercage of the REUSY by using the NH₃-TPD and Py-FTIR spectra techniques (*cf.* Fig. S2 and S3). In the protonation of 2-methylthiophene, the protonated products have two possibilities. The one forms tertiary carbenium ion existing p- π and σ -p conjugated, and another generates secondary carbenium ion. According to the previous literatures reported [19], although the relative stabilities of the tertiary carbenium ion is more stable, the secondary carbenium ion has higher activities in the next oligomerization. Hence, the protonated 2-methylthiophene with the secondary carbenium ion possibly attack the 2- or 5-position of the 2-methylthiophene molecules adsorbed on the AlO⁺ active sites in the HY, or on the Al(OH)²⁺ and RE(OH)²⁺ active sites in the REUSY, and then form the 2-methylthiophene dimers. Sub-

sequently, the carbenium ion has selectivity from the dimers to the trimers that can only attack the 5-position of the adsorbed 2-methylthiophene molecules, rather than the 2-position. Ultimately, the 2-methylthiophene trimers can be obtained [*cf.* Fig. 5(a) and (b)]. For 3-methylthiophene, the protonated products with the carbenium ion located in the 5-position of 3-methylthiophene molecules have higher activities in the next oligomerization. However, the protonated 3-methylthiophene dimers don't have higher selectivity which can both attack 2- or 5-position of the adsorbed 3-methylthiophene molecules and then possibly generate the 3-methylthiophene trimers (*cf.* Fig. 3, k3 and k4). The Fig. 5 (c) and (d) show the formation processes of the k3 trimers on that active sites in the HY and REUSY, and meanwhile, the k4 trimers can follow the forming pathways of the k3 trimers.

Apart from the trimers detected above, however, some other sulfur compounds are also observed, mainly including the methylthiophene dimers (d, e and f), the trimers derivatives (j) and the cracked products (a, b, c, g, h, and i) (*cf.* Fig. 3, inset). It can be found that, in the inset, the concentrations of the abovementioned sulfur compounds trapped on the REUSY are more than that on the HY, but are obviously lower than that of the trimers, indicating that not only the oligomerization reaction of the methylthiophene molecules can occur on the HY and REUSY, but also there is a weaker cracking reaction and the cracking abilities are stronger on those active sites in the REUSY, implying that the OH active sites of Si and Al atoms located in the REUSY also can improve the cracking abilities of the trimers. In addition, the concentrations of the 3-methylthiophene dimers (d, e and f) are higher than that of the 2-methylthiophene dimers. The concentration of the c sulfur compound after 3-methylthiophene adsorbed on the zeolites is more than that of 2-methylthiophene, while the concentrations of the a, b, g, h and i sulfur compounds after 2-methylthiophene

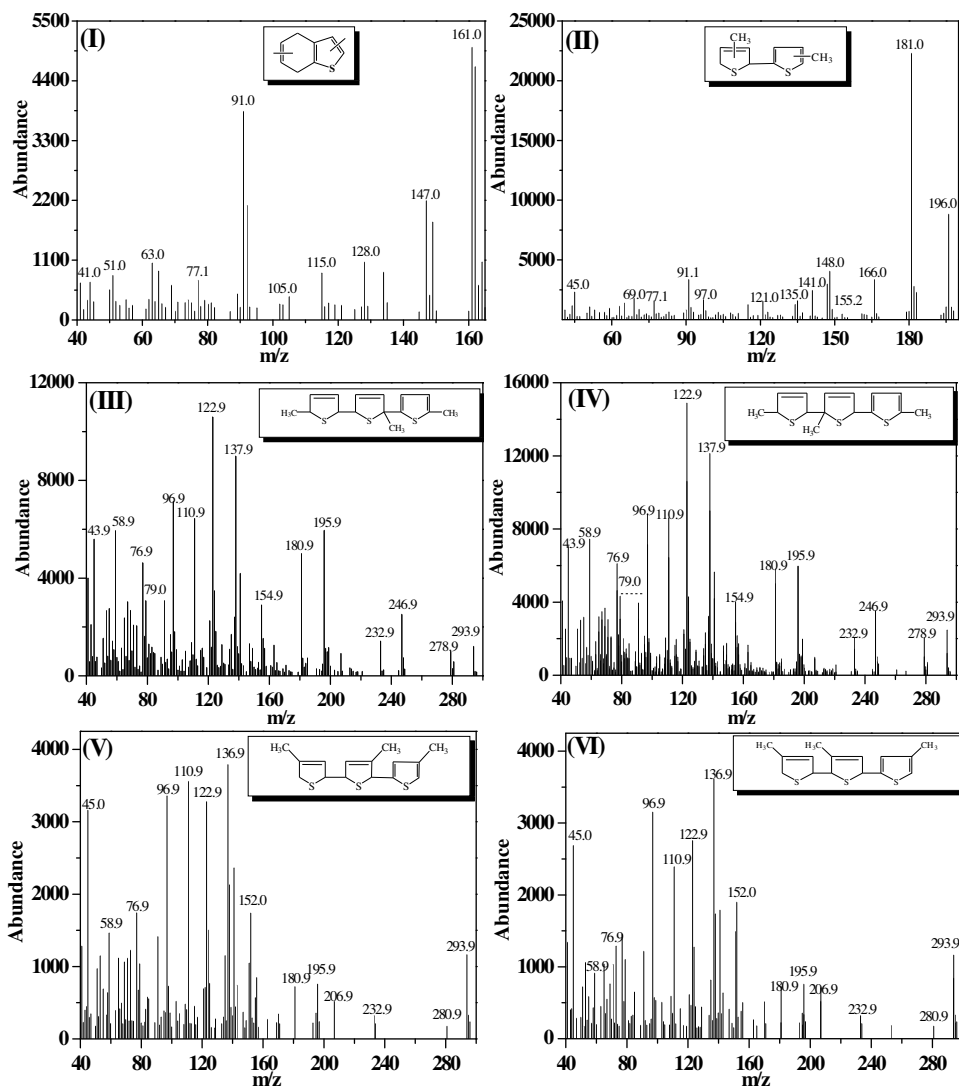


Fig. 4. Mass spectrum of the cracked products c-(I), the methylthiophene dimers f-(II), the 2-methylthiophene trimers k1-(III), k2-(IV) and the 3-methylthiophene trimers k3-(V), k4-(VI).

adsorbed on the zeolites is higher than that of 3-methylthiophene. Here, the chemical structures of the 2-methylthiophene and 3-methylthiophene trimers (*cf.* Table 2S, k1, k2, k3, and k4) are the main reason that lead to the difference of the distribution and concentrations of these sulfur compounds.

In addition, system temperatures also play an important role in the oligomerization and cracking processes, as stated the FTIR spectra analysis. In the GC-SCD chromatograms, just the a, b, c, d, and i sulfur compounds are observed as system temperature is up to 373 K. The methylthiophene trimers cannot be found. Surprisingly, this phenomenon is not consistent with the results of the corresponding FTIR spectra in which the oligomerization reaction of the methylthiophene molecules can occurs further (*cf.* Fig. 1(A, 2), (A, 3), (B, 2) and (B, 3), line c). This is also different from the literatures reported that the abilities of proton transfer in the OH active sites of the Si and Al atoms located in the zeolites strengthened with the temperature rising [19], which may result in the protonated trimers further occur the oligomerization by combining with the adjacent adsorbed methylthiophene molecules continually. Hence, it can be reasonably explained that the oligomers with higher boiling point may be formed which cannot be detected in the GC-SCD chromatograms, such as the tetramers, etc. Naturally, these kinds of oligomers may be more

stable and complicated than that of the trimers. It can be known that, therefore, the oligomers may be originated from the protonated trimers, as exemplified in the k2 and k3, combining with the adsorbed methylthiophene molecules unceasingly (*cf.* Fig. 6). Like the formation process of the 2-methylthiophene and 3-methylthiophene trimers, the stronger oligomerization abilities are still associated with the RE(OH)²⁺ active sites in the REUSY. At this moment, however, not only the protonation abilities of 2-methylthiophene and 3-methylthiophene should be considered as an crucial factor, but also the pore diameter distribution of the zeolitic supercages determine the polymeric degree (n) of the methylthiophene molecuels. Especially, the oligomerization abilities of 2-methylthiophene on the zeolites are particularly outstanding, which have been reflected in the FTIR spectra analysis results at degassing temperature of 373 K (*cf.* Fig. 1(A, 2), (A, 3), (B, 2) and (B, 3), line c).

Furthermore, the cracking abilities of those oligomers are also different. For 2-methylthiophene, the content of the a and i sulfur compounds increase, and the b, c and d sulfur compounds decrease. While for 3-methylthiophene, the a sulfur compound also increase, and the b and c sulfur compounds decrease obviously. Like the cracking of the 2-methylthiophene or 3-methylthiophene trimers, these results are most possibly attributed to different chemi-

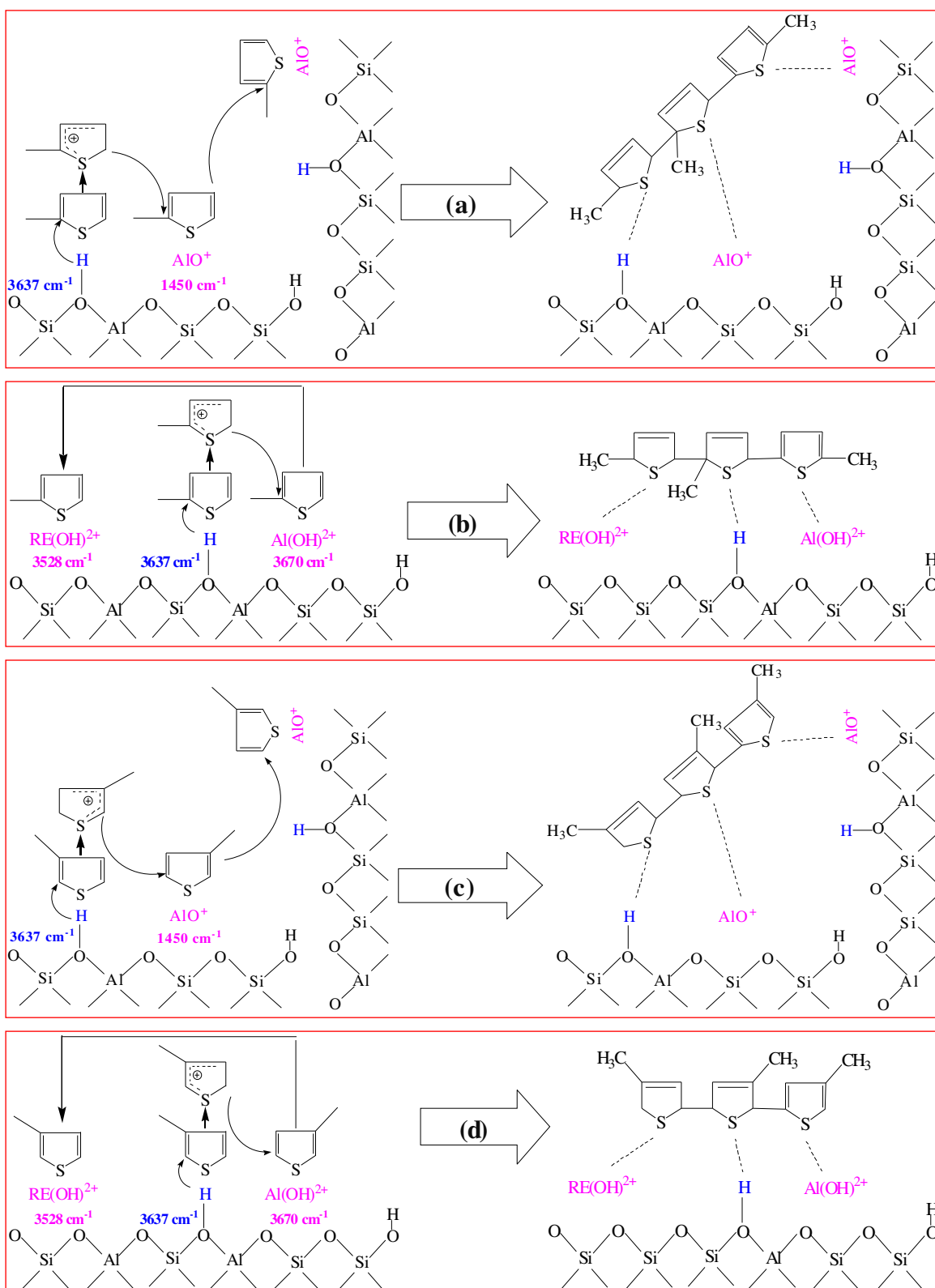


Fig. 5. Oligomerization processes of 2-methylthiophene and 3-methylthiophene adsorbed on the active sites in the HY and REUSY at temperature of 303 K. (a): 2-methylthiophene adsorbed on the HY, (b): 2-methylthiophene adsorbed on the REUSY, (c): 3-methylthiophene adsorbed on the HY, (d): 3-methylthiophene adsorbed on the REUSY.

cal structures of the 2-methylthiophene and 3-methylthiophene oligomers (*cf.* Fig. 6). As for, the cracking processes of the methylthiophene oligomers need to be further studied, due to their inconclusive chemical structures.

As system temperature is up to 473 K, few sulfur compound can be found in the GC-SCD chromatograms. And even, no sulfur compounds can be observed at system temperature of 573 K. Combined with the results of the corresponding FTIR spectra anal-

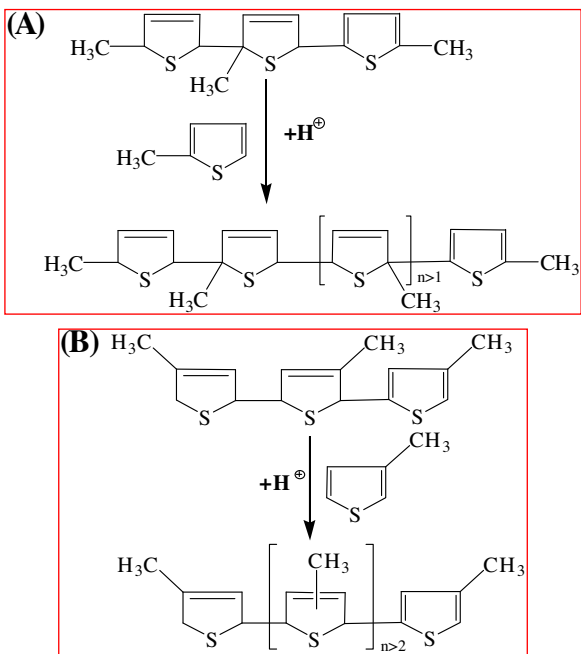


Fig. 6. Further oligomerization processes of 2-methylthiophene (A) and 3-methylthiophene (B) adsorbed on the active sites in the HY and REUSY at temperature of 373 K.

ysis (cf. Fig. 1(A, 2), (A, 3), (B, 2) and (B, 3), the lines d and e), the bands of 1515 and 1527 cm^{-1} disappear thoroughly. Hence, it can be inferred that the oligomerization reaction of the methylthiophene molecules hardly occur at system temperatures of $> 473\text{ K}$. Oppositely, the cracking reaction is accelerated, and moreover, the cracking degree is very heavier, compared to the cracking reaction at the system temperatures of 303 and 373 K.

In conclusions, the abovementioned results systematically demonstrate the roles of each active site in the NaY, HY and REUSY for adsorption-transformation behaviors of the methylthiophene molecules by the FTIR spectra and the distribution of the sulfur compounds species trapped on the zeolites. The adsorptive modes

and abilities of the relevant active sites in the NaY, HY and REUSY, and especially the cracking processes of the trimers, however, need us to investigate further.

3.3. Cracking mechanisms

Figs. 7–9 provide the TG-DTG profiles and the MS signals curves of the desorbed products detected during the TPD processes. It can be found that, for the DTG profiles of the methylthiophene molecules on the NaY, only one temperature desorption signal peak is observed at temperatures of *ca.* 398 and 388 K, respectively [cf. Fig. 7(A, 1) and (A, 2)]. This desorption peak is ascribed to the desorption of the adsorbed methylthiophene molecules which can be approved by the MS signal change of the methylthiophene molecules ($m/z = 97, 98$) and H_2S ($m/z = 34$) detected [cf. Fig. 7(B, 1) and (B, 2)]. For the H_2S ($m/z = 34$), no signal can be found in the MS signal of the desorbed products. These findings indicate that the adsorption interaction between the methylthiophene molecules and the NaY is relatively weaker, which is consistent with the conclusion obtained from the FTIR spectra (cf. Fig. 1(A, 1) and (B, 1)) discussed above.

Compared to the adsorption-transformation behaviors of the methylthiophene molecules adsorbed on the NaY, the DTG profiles of the methylthiophene molecules on the HY and REUSY, and the MS signals change of the desorbed products are relatively complicated (cf. Figs. 7–9). Two temperature desorption signal peaks can be observed for all the systems. For the low temperature signal peaks [cf. Figs. 7–9(A, 1) and (A, 2)], the desorption temperatures of *ca.* 423 and 453 K after 2-methylthiophene and 3-methylthiophene adsorbed on the HY, respectively, are slightly higher than the corresponding desorption temperatures of *ca.* 409 and 431 K after that on the REUSY, and all are slightly higher than that on the NaY. In addition, the desorption temperatures (*ca.* 453 and 431 K) after 3-methylthiophene adsorbed on the zeolites, respectively, are slightly higher than the corresponding desorption temperatures (*ca.* 423 and 409 K) of 2-methylthiophene. These slight difference mainly originate from adsorptive interaction between the OH active sites of the Si and Al atoms in the supercage of the zeolites Y and the methylthiophene molecules, that is, the easier the protonation, the lower the desorption temperature.

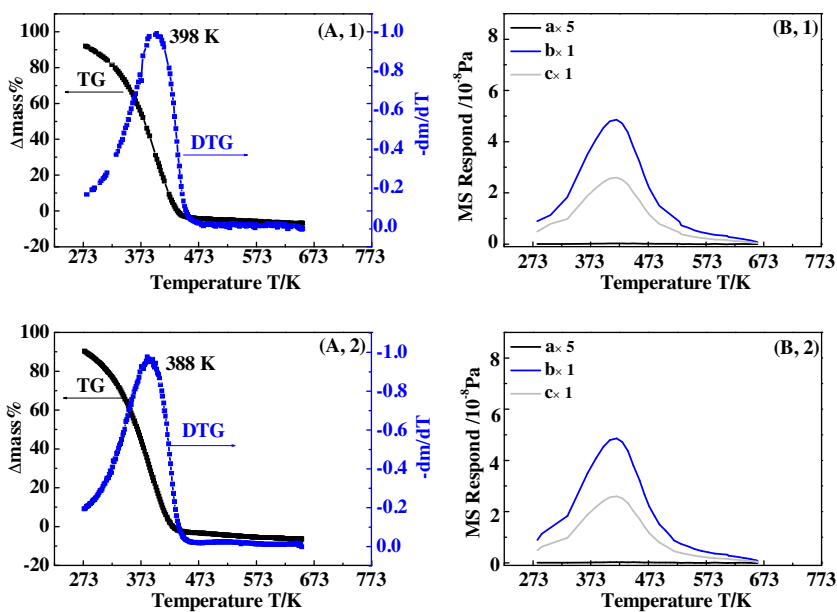


Fig. 7. TG-DTG profiles (A) of 2-methylthiophene (1) and 3-methylthiophene (2) adsorbed on the NaY and the MS detected signals curves (B) of the desorbed products during the TPD. a- H_2S ($m/z = 34$), b, c-methylthiophenes ($m/z = 97, 98$); “a $\times 5$ ” denotes the magnified times of the MS signals of the H_2S and the MS signals of the others are the same.

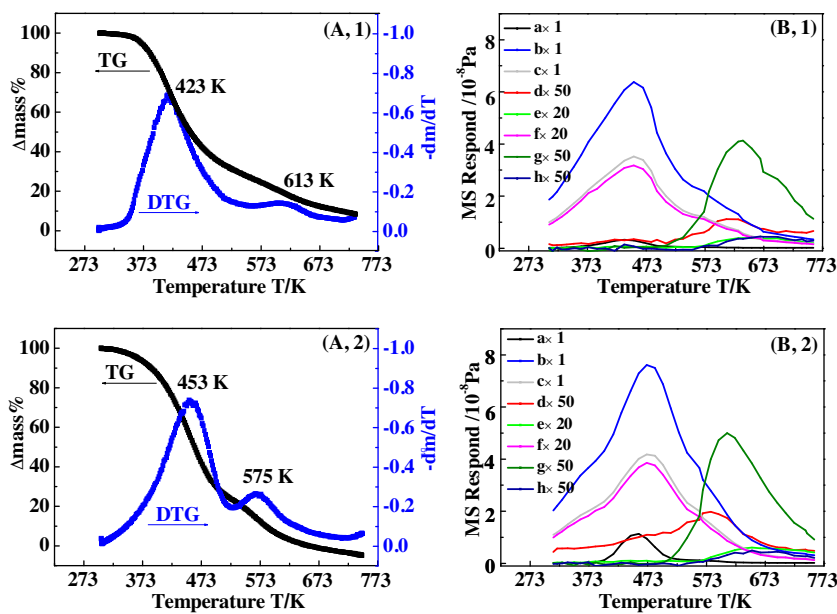


Fig. 8. TG-DTG profiles (A) of 2-methylthiophene (1) and 3-methylthiophene (2) adsorbed on the HY and the MS detected signals curves (B) of the desorbed products during the TPD. a-H₂S ($m/z=34$), b, c-methylthiophenes ($m/z=97, 98$), d-thiophene ($m/z=84$), e-alkylbenzene ($m/z=91$), f-methyldihydrothiophenes ($m/z=100$), g-dimethylthiophenes ($m/z=112$), h-alkylthiophenes ($m/z=126$).

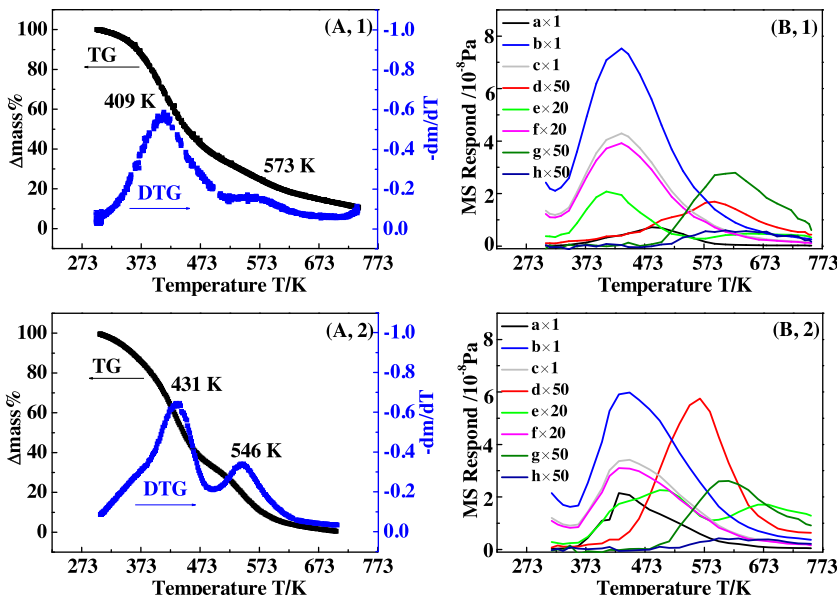


Fig. 9. TG-DTG profiles (A) of 2-methylthiophene (1) and 3-methylthiophene (2) adsorbed on the REUSY and the MS detected signals curves (B) of the desorbed products during the TPD.

Meanwhile, in combination with the corresponding MS signals analysis, apart from the strong MS signal of the adsorbed methylthiophene molecules ($m/z=97, 98$) during the TPD process, some new and weak MS signals of $m/z=34, 91, 100$ are also observed [cf. Figs. 7–9(B, 1) and (B, 2)]. The stronger MS signals of the adsorbed methylthiophene molecules ($m/z=97, 98$) implies that some protonated 2-methylthiophene and 3-methylthiophene molecules can be desorbed from the OH active sites of the Si and Al atoms in the supercage of the HY and REUSY, which is supported each other with the weakening of the bands at 1436 and 1454 cm^{-1} (cf. Fig. 1(A, 2), (A, 3), (B, 2) and (B, 3), line b). Besides, the new MS signals of $m/z=34, 91, 100$ observed indicate that some transformation processes of the methylthiophene molecules occur in the systems. It can be known that, therefore, the new MS signals can be ascribed

to the products of the initial cracking of the trimers, which have been detected in the GC-SCD chromatograms (cf. Fig. 3).

Based on the analysis of the abovementioned results, the initial cracking processes of the 2-methylthiophene and 3-methylthiophene trimers, as exemplified in the k₂ and k₃, are speculated by the detected signals of H₂S ($m/z=34$), alkylbenzene ($m/z=91$) and methyldihydrothiophenes ($m/z=100$), and the sulfur compounds species retained on the HY and REUSY (cf. Fig. 10a). In these MS signals, the MS signals change of the H₂S and alkylbenzene on the REUSY are stronger than that on the HY, well proving that the cracking abilities of the methylthiophene trimers are easier on the stronger acidic intensities of the OH active sites caused by the Al(OH)²⁺ and RE(OH)²⁺ active sites in the REUSY than that caused by the AlO⁺ active sites in the HY discussed above. As

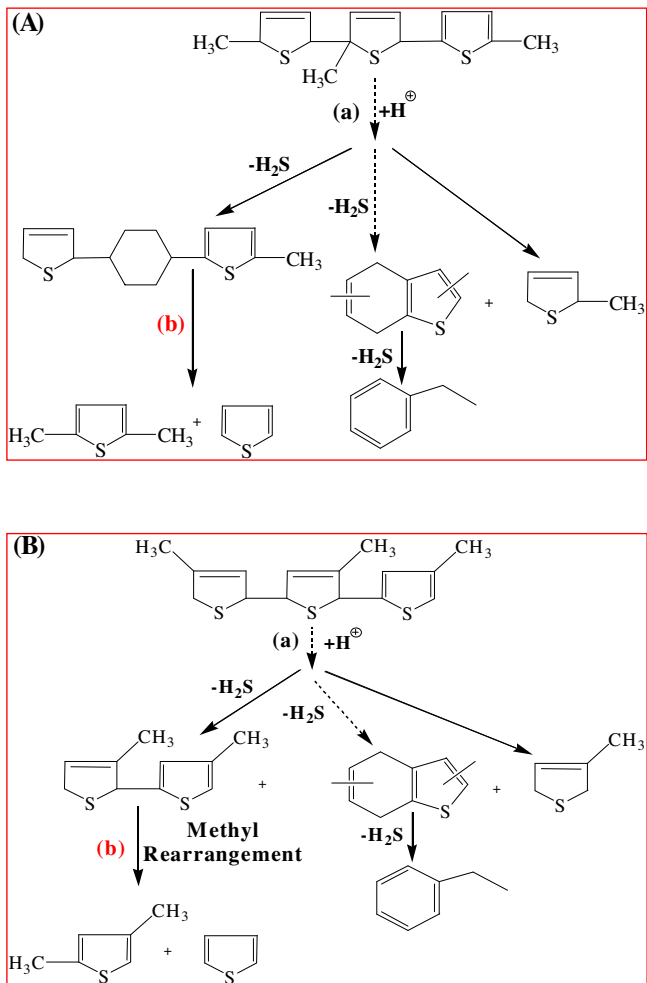


Fig. 10. Cracking processes of the 2-methylthiophene (A) and 3-methylthiophene (B) trimers on the HY and REUSY.

for, the MS signal change of the H₂S from the cracking of the 3-methylthiophene trimers is stronger than that from the cracking of the 2-methylthiophene trimers. The result shows that the chemical structures of the 2-methylthiophene trimers slightly are more complicated than that of the 3-methylthiophene trimers, eventually resulting in the cracking abilities of the 2-methylthiophene trimers with relatively weaker.

Similarly, for the high temperature signal peaks, the desorption temperatures of *ca.* 613 and 575 K after 2-methyl- and 3-methylthiophene adsorbed on the HY, respectively, are higher than that of *ca.* 573 and 546 K after that on the REUSY. The result is still related to the protonation abilities of the methylthiophene molecules on the HY and REUSY zeolites. Unusually, the desorption temperatures (*ca.* 613 and 573 K) after 2-methylthiophene adsorbed on the zeolites are higher than that (*ca.* 575 and 546 K) of 3-methylthiophene. In addition, the desorption signal peaks of 2-methylthiophene are broader than that of 3-methylthiophene. At this moment, the chemical structures of the products after the initial cracking of 2-methylthiophene and 3-methylthiophene trimers at low temperature desorption, are considered as the main influential factor.

In the corresponding MS detected signals of desorbed products during the TPD processes, except for some other new and very weak MS signals of *m/z* = 84 (thiophene), 112 (dimethylthiophenes) and 126 (alkylthiophenes) detected, the MS signals of the methylthiophene molecules (*m/z* = 97, 98) and the H₂S (*m/z* = 34) cannot be found, and all the MS signals strength decreases obviously, com-

pared to that at the low temperature signal peaks, confirming that these new weaker MS signals are from the further cracking of the cracked products after the methylthiophene trimers cracked at low desorption temperature (*cf.* Fig. 10b). Remarkably, the MS signal of the thiophene are stronger on the REUSY than that on the HY, while the MS signals of the dimethylthiophenes on the REUSY are slightly weaker than that of on the HY. Besides, the MS signals of the thiophene from the cracking of the 3-methylthiophene trimers are stronger than that of the 2-methylthiophene trimers, still due to different chemical structures of the cracked products after the cracking of the 2-methylthiophene or 3-methylthiophene trimers.

According to the results analyzed and discussed above, the formation of the methylthiophene trimers, tetramers or more complicated oligomers confirm that the removal of the methylthiophene molecules is mainly restrained by the effects of the relevant active sites of the zeolite-based sorbents, rather than are entirely caused by the influences of steric hindrance of the zeolite-based sorbents [20,21] and eventually result in the application of selective adsorption desulfurization process became difficult in deep desulfurization for FCC naphtha in the future.

Insight into the correlation between adsorption-transformation behaviors of 2-methylthiophene and 3-methylthiophene and the active sites of the NaY, HY and REUSY, two directions can be considered in the deeply removing the methylthiophenes or even other thiophenic sulfur compounds in FCC naphtha, and the design of the sorbents in the future. The one is that the OH active sites of the Si and Al atoms in acidic catalysts should be inhibited, mainly avoiding the acid catalyzed condensation reactions occurred and needing to enhance the adsorptive abilities of the adsorptive active sites (e.g. AlO⁺, Al(OH)²⁺, or RE(OH)²⁺, etc.), which can improve the adsorptive sulfur capacity and selectivity for ultra-deep adsorption desulfurization process. Another is that the acidic intensity and decrease the density of the OH active sites of the Si and Al atoms should be enhanced and reduce the adsorptive active sites on the acid catalysts so that the dimers, trimers or teramers, etc. can convert into H₂S directly for in situ sulfur removal in FCC process or make the methylthiophene molecules transfer into long chain alkylthiophenes by combining with the olefins of FCC naphtha in OATS process. Apart from the modulation of the relevant active sites of the zeolite-based sorbents, however, system temperatures also will be worth to ponder over, facilitating the cracking of that oligomers.

4. Conclusions

In this work, the roles of each active site in the NaY, HY and REUSY zeolites interacted with the methylthiophene molecules are confirmed. For the NaY, the thiophene-ring of the adsorbed methylthiophenes is parallel to the Na⁺ active sites by π electron interaction. For the HY and REUSY, the bridging hydroxyl (OH) groups of the Si and Al atoms located in the supercage of zeolites Y are the preferred active sites, leading to the protonation and cracking reactions of the methylthiophene molecules. The AlO⁺ active sites in the HY, and the Al(OH)²⁺ and RE(OH)²⁺ active sites in the REUSY both can make the oligomerization reaction occur at 303 and 373 K, and especially, the RE(OH)²⁺ active sites significantly improve the oligomerization abilities. The activities and selectivities of the protonated 2-methylthiophene result in that the oligomerization abilities are stronger than that of 3-methylthiophene, but the cracking abilities are contrary. As system temperatures of > 473 K, the oligomerization reaction is restricted, while the cracking reaction is accelerated. Thereby, modulation of the key active sites and system temperatures will be a good prospect for ultra-deep desulfurization in the future.

Acknowledgements

This work is financially supported by the National Natural Science Foundation of China (Nos. 21076100 and 21376114) and by the China National Petroleum Corporation (Grant No. 10-01A-01-01-01).

Appendix A. Supplementary data

Supplementary data associated with this article can be found, in the online version, at <http://dx.doi.org/10.1016/j.apcatb.2016.10.008>.

References

- [1] C. Marcilly, Stud. Surf. Sci. Catal. 135 (2001) 37–60.
- [2] C. Yin, G. Zhu, D. Xia, Fuel Process. Technol. 79 (2) (2002) 135–140.
- [3] J.T. Miller, W.J. Reagan, J.A. Kaduk, C.L. Marshall, A.J. Kropf, J. Catal. 193 (2000) 123.
- [4] C. Yin, G. Zhu, D. Xia, Am. Chem. Soc. Prepr. Div. Pet. Chem. 47 (4) (2002) 391.
- [5] C. Yin, G. Zhu, D. Xia, Am. Chem. Soc. Prepr. Div. Pet. Chem. 47 (4) (2002) 398.
- [6] A. Corma, C. Martinez, G. Ketley, G. Blair, Appl. Catal. A: Gen. 208 (2001) 135.
- [7] P. Leflaive, J.L. Lemberton, G. Pérot, C. Mirgaine, J.Y. Carriat, J.M. Colin, Stud. Surf. Sci. Catal. 130 (2000) 2465–2470.
- [8] P. Leflaive, J.L. Lemberton, G. Pérot, C. Mirgaine, J.Y. Carriat, J.M. Colin, Appl. Catal. A: Gen. 227 (1) (2002) 201–215.
- [9] X. Ma, S. Velu, J.H. Kim, C. Song, Appl. Catal. B: Environ. 56 (1) (2005) 137–147.
- [10] B.D. Alexander, G.A. Huff, V.R. Pradhan, W.J. Reagan, R.H. Clayton, US Patent 6,024,865 (2000).
- [11] J.A. Valla, A.A. Lappas, I.A. Vasalosa, C.W. Kuehler, N.J. Gudded, Appl. Catal. A: Gen. 276 (2004) 75–87.
- [12] C. Song, Catal. Today 86 (1) (2003) 211–263.
- [13] R.T. Yang, A. Takahashi, F.H. Yang, Ind. Eng. Chem. Res. 40 (26) (2001) 6236–6239.
- [14] K.X. Lee, J.A. Valla, Appl. Catal. B: Environ. 201 (2017) 359–369.
- [15] S. Velu, X. Ma, C. Song, Ind. Eng. Chem. Res. 42 (2003) 5293–5304.
- [16] Y. Shi, W. Zhang, H. Zhang, F. Tian, C. Jia, Y. Chen, Fuel Process. Technol. 110 (2013) 24–32.
- [17] Y. Qin, Z. Mo, W. Yu, S. Dong, L. Duan, X. Gao, L. Song, Appl. Surf. Sci. 292 (2014) 5–15.
- [18] D. Richardieu, G. Joly, C. Canaff, P. Magnoux, M. Guisnet, M. Thomas, A. Nicolaos, Appl. Catal. A: Gen. 263 (1) (2004) 49–61.
- [19] H. Shan, C. Li, C. Yang, H. Zhao, B. Zhao, J. Zhang, Catal. Today 77 (1) (2002) 117–126.
- [20] T. Boita, M. Moreau, F. Richard, G. Pérot, Appl. Catal. A: Gen. 305 (1) (2006) 90–101.
- [21] F. Richard, T. Boita, M. Moreau, C. Bachmann, G. Pérot, J. Mol. Catal. A: Chem. 273 (1) (2007) 48–54.
- [22] Y. Wen, G. Wang, C. Xu, J. Gao, Energy Fuel 26 (2012) 3201–3211.
- [23] X. Pang, L. Zhang, S. Sun, T. Liu, X. Gao, Catal. Today 125 (2007) 173–177.
- [24] O.V. Potapenko, V.P. Doronin, T.P. Sorokina, V.P. Talsi, V.A. Likholobov, Appl. Catal. B: Environ. 117–118 (2012) 177–184.
- [25] O.V. Potapenko, V.P. Doronin, T.P. Sorokina, V.A. Likholobov, Fuel Process. Technol. 128 (2014) 251–256.
- [26] C. Zhang, Y. Qin, X. Gao, H. Zhang, Z. Mo, C. Chu, X. Zhang, L. Song, Acta Phys.-Chim. Sin. 31 (2) (2015) 344–352.
- [27] S. Li, A. Zheng, Y. Su, H. Zhang, L. Chen, J. Yang, C. Ye, F. Deng, J. Am. Chem. Soc. 129 (36) (2007) 11161–11171.
- [28] S. Li, A. Zheng, Y. Su, H. Fang, W. Shen, Z. Yu, L. Chen, F. Deng, Phys. Chem. Chem. Phys. 12 (15) (2010) 3895–3903.
- [29] C. Mirodatos, D. Barthomeuf, J. Chem. Soc. Chem. Commun. 2 (1981) 39–40.
- [30] J. Li, P. Zeng, L. Zhao, S. Ren, Q. Guo, H. Zhao, B. Wang, H. Liu, X. Pang, X. Gao, B. Shen, J. Catal. 329 (2015) 441–448.
- [31] A.J. Hernández-Maldonado, F.H. Yang, G. Qi, R.T. Yang, Appl. Catal. B: Environ. 56 (2005) 111–126.
- [32] J.W. Ward, Trans. Faraday Soc. 67 (1971) 1489–1499.
- [33] A.J. Hernández-Maldonado, R.T. Yang, Ind. Eng. Chem. Res. 42 (2003) 123–129.
- [34] K.A. Layman, M.E. Bussell, J. Phys. Chem. B 108 (40) (2004) 15791–15802.
- [35] H. Hogeweij, Recl. des Trav. Chim. des Pays-Bas 85 (10) (1966) 1072–1076.
- [36] S.L. Meisel, G.C. Johnson, H.D. Hartough, J. Am. Chem. Soc. 72 (5) (1950) 1910–1912.
- [37] A. Ishigaki, T. Shono, B. Chem. Soc. Jpn. 48 (10) (1975) 2977–2978.